Progress In Electromagnetics Research B, Vol. 39, 319–335, 2012

AMPLITUDE AND DIRECTIONAL OF ARRIVAL ESTIMATION: COMPARISON BETWEEN DIFFERENT TECHNIQUES

F. Zaman[1,*], I. M. Qureshi[2], A. Naveed[3], J. A. Khan[1], and R. M. A. Zahoor[1]

[1]Department of Electronic Engineering, International Islamic University, H-10, Islamabad, Pakistan

[2]Electrical Department, Air University, Islamabad, Pakistan

[3]School of Engineering & Applied Science, Isra University, Islamabad, Pakistan

Abstract—In this work, we propose a method based on Genetic algorithm hybridized with Pattern Search for joint estimation of Amplitude and Direction of Arrival, azimuth as well as elevation angles using L-type array. Four other schemes, i.e., the Genetic algorithm, Pattern Search, Simulated Annealing and Simulated Annealing hybridized with Pattern Search are also discussed and compared with Genetic algorithm hybridized with Pattern Search. Multiple sources are taken in the far field of sensors array and Mean Square Error is taken as a fitness function. This fitness function is optimal in nature and requires only a single snapshot. It avoids any ambiguity or required permutation as in some other methods to link it with angles found in the previous snapshot. The reliability and effectiveness of the proposed scheme is tested on the basis of Monte-Carlo simulations and its statistical analysis.

1. INTRODUCTION

Recently, one of the dynamic research areas in electromagnetic and wireless communication systems is smart antenna. The demand of smart antenna drastically increases when dealing with multi-user communication system, which needs to be adaptive, especially in unknown time varying scenarios [1]. Adaptive or smart antennas

Received 21 February 2012, Accepted 19 March 2012, Scheduled 26 March 2012

* Corresponding author: Fawad Zaman (fawad.phdee31@iiu.edu.pk).

system consists of an array of radiating sensors. These array sensors are quite able to steer the main beam in any desired direction in space [2], while placing a suitable null in the direction of unwanted signals or jammers [3–5]. In this connection, Direction of Arrival (DOA) estimation of received signal is one of the fundamental and necessary steps to construct a smart or adaptive receiver. DOA estimation of sources impinging on an array of sensors has numerous applications in the field of radar, sonar and wireless communication system [6, 7]. The two dimensional DOA estimation of sources has been a focusing area of researchers since last two decades. The 2-D, DOA estimation requires two dimensional array such as Planar array, L-type array etc. In [8], planar array is used for 2-D DOA estimation of sources while in [9] two parallel uniform linear arrays have been used. In [10, 11] L-type arrays have been used for the same problem.

In today's development, no one can decline the importance of meta-heuristic techniques like Genetic algorithms (GAs), Particle Swarm optimization (PSO) etc. It is well acknowledged that these techniques are quite successful, reliable and efficient. In research community, the GA especially, has achieved much attention because of its ability of decision making and autonomous learning. The most fascinating reason due to which GA has been widely studied is its robustness during optimization and searching [12]. In [13], the multi-layered perceptrons based on Radial Basis Function Neural Network (RBFNN) have been used to estimate DOA of mobile users, using linear antenna arrays. In this, the strength of Hopfield neural networks (HNN) has been exploited for the DOA estimation. In [14] hybrid approach, i.e., the neural networks and ant-colony optimization has been used for estimating DOA of sources impinging on linear array. In [15] GA has been used for 2-D DOA estimation based on maximum likelihood technique for uniform circular array. However, the hybrid approach based on evolutionary computation along with any efficient hybrid function, i.e., Pattern Search (PS), Active Search (AS) etc. is an area to be explored.

In this paper, according to the best of our knowledge, no one has yet applied intelligent hybrid computing for joint estimation of Amplitude and Direction of Arrival (azimuth and elevation angles) of sources impinging on L-type array. Four other schemes, i.e., the Genetic algorithm (GA), Pattern Search (PS), Simulated Annealing (SA) and Simulated Annealing hybridized with Pattern Search (SA-PS) are also discussed and compared with GA hybridized with Pattern Search (GA-PS). Multiple sources have been taken in the far field of sensors array and Mean Square Error is taken as a fitness function. This fitness function is optimal in nature and requires only a single snapshot. The association of new estimates with targets is the key issue in multiple targets tracking system. N targets imply $N!$ possible combination which requires some computations [16]. In using mean square error (MSE) as fitness function, the new estimation of DOAs is automatically linked with old estimation of angles from previous snapshot which decreases the computational complexity [17]. Moreover, L-type array has been used which is composed of two uniform linear arrays, i.e., one linear array is along X-axis and the other is along Z-axis. Both the uniform linear arrays consist of same number of antenna elements while the reference element is common for both of them. The reliability and effectiveness of the proposed scheme has been tested on the basis of Monte-Carlo simulations and its statistical analysis.

This paper is organized as follows: In Section 2, we provide the data model about amplitude and DOA estimation for L-type array. In Section 3, we describe the learning methodology for joint amplitude and DOA of sources. Section 4, is devoted for simulation and results, while Section 5 gives conclusion and future work direction.

2. DATA MODEL

Consider P narrow band sources impinging from different directions from far field on L-type array. The L-type array consists of two uniform linear arrays, i.e., one along X-axis and the other along Z-axis. Each linear array has M elements while the reference element is common for both arrays as shown in Fig.1 [18]. Both the arrays have same inter-

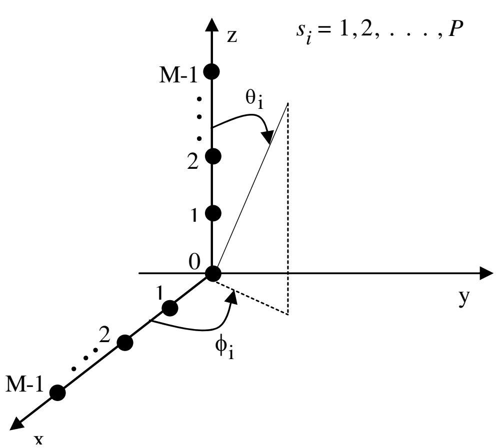

Figure 1. L-type array having two uniform linear arrays.

element spacing d. The signals are narrow band with known frequency ω_o. Assume that the ith signal received on sensor array has amplitude s_i, elevation angle θ_i and azimuth angle ϕ_i where $i = 1, 2, \ldots P$. The appropriate observed signal on sub-array along X-axis, $\mathbf{y}_x$ and sub-array along Z-axis, $\mathbf{y}_z$ is given as

$$\mathbf{y}_x = \mathbf{B}_x(\theta,\phi)\mathbf{s} + \boldsymbol{\mu}_x = \sum_{i=1}^{P} \mathbf{b}_x(\theta_i,\phi_i)s_i + \boldsymbol{\mu}_x \tag{1}$$

$$\mathbf{y}_z = \mathbf{B}_z(\theta)\mathbf{s} + \boldsymbol{\mu}_z = \sum_{i=1}^{P} \mathbf{b}_z(\theta_i)s_i + \boldsymbol{\mu}_z \tag{2}$$

where

$$\begin{aligned}
\mathbf{y}_x &= [y_{x,0}, y_{x,1}, \ldots y_{x,M-1}]^T,\\
\mathbf{y}_z &= [y_{z,0}, y_{z,1}, \ldots y_{z,M-1}]^T,\\
\mathbf{s} &= [s_1, s_2, s_3, \ldots s_P]^T\\
\boldsymbol{\mu}_x &= [\mu_{x,0}, \mu_{x,1}, \ldots \mu_{x,M-1}]^T,\\
\mathbf{B}_x(\theta,\phi) &= [\mathbf{b}_x(\theta_1,\phi_1), \mathbf{b}_x(\theta_2,\phi_2), \ldots \mathbf{b}_x(\theta_P,\phi_P)]^T,\\
\mathbf{B}_z(\theta) &= [\mathbf{b}_z(\theta_1), \mathbf{b}_z(\theta_2), \ldots \mathbf{b}_z(\theta_P)]^T,
\end{aligned}$$

where

$$\begin{aligned}
\mathbf{b}_x(\theta_i,\phi_i) &= [1 \exp(-j\psi_{x,i}) \ldots \exp(-j(M-1)\psi_{x,i})]^T,\\
\mathbf{b}_z(\theta_i) &= [1 \exp(-j\psi_{z,i}) \ldots \exp(-j(M-1)\psi_{z,i})]^T,
\end{aligned}$$

$\psi_{x,i} = 2\pi(d/\lambda)\sin\theta_i\cos\phi_i$ and $\psi_{z,i} = 2\pi(d/\lambda)\cos\theta_i$, where $i = 1, 2, \ldots P$. $\mathbf{b}_x(\theta, \phi)$ and $\mathbf{b}_z(\theta)$ denote the steering vector along the X-axis sub-array and along the Z-axis sub-array. $\boldsymbol{\mu}_x$ and $\boldsymbol{\mu}_z$ represent the circular complex valued noise vector added at the output of X-axis sub-array and Z-axis sub-array, respectively. As shown in (1) and (2) the unknown parameters are the amplitudes s_i, the elevation angle θ_i and the azimuth angle ϕ_i where $i = 1, 2, \ldots P$. Here the problem in hand is joint estimation of amplitudes and DOA of sources by using intelligent hybrid computing approach.

3. PROPOSED METHODOLOGIES

In this section, a brief introduction, flow diagram, and parameter setting used for joint estimation of amplitude and DOA of sources are given for GA, PS and SA algorithms. Simulated annealing (SA) method was first of all introduced in 1950 by Metropolis, in which the process for crystallization model is explained. However, proper research on SA has been carried out by Kirkpatric et al. [19]. Basically, SA is a probabilistic computational technique used for the local and global optimization problems based on modeling of materials having controlled cooling and heating properties. The core objective of SA is to find out the candidate solution efficiently and effectively in fixed amount of time. In many optimization problems, the condition of differentiability, convexity and continuity is required, while SA technique does not need it, which is its main advantage. Many researchers used SA in diverse field of engineering, like the transmission network expansion planning problem, 3D face recognition and unit commitment problems [20–22].

Pattern Search (PS) technique is also used for optimization which does not need the gradient of the problem. The main goal of PS technique is to compute a sequence of points that reach an optimal point. In each step, the technique tries to find out a set of points called mesh around the optimal point of previous step. The mesh can be obtained by adding the current point to a scalar multiple of vectors called a pattern [23]. The new point becomes the current point in the next step of algorithm, if the PS finds out the point in the mesh that improves the objective function at the current point. PS method is very successful for optimization problem such as, Bound constrained minimization and Globaly Convergent Augmented Lagrangian algorithm [24].

The GA was introduced by John H. Holland in 1975 in his work to present a simple solution of natural selection [25]. GA belongs to a large family of evolutionary computing inspired by natural phenomena and is more reliable technique than any other heuristic mathematical solvers. [26, 27]. Due to the simplicity in concept, ease in implementation and less probability of getting stuck in local minima, GA has been used in various applications of array signal processing [28], communication [29] and soft computing [30].

By keeping in mind the importance of SA, PS and GA, we will use these techniques for joint estimation of amplitude and DOA of sources. Moreover, we will also use the hybrid approach such as GA-PS, SA-PS for further tuning of our results. The generic flow diagram for joint estimation of amplitude and DOA of sources is shown in Fig. 2.

In this paper, we have used the MATLAB optimization toolbox for GA, PS and SA for estimation of amplitudes and DOA of sources with the setting shown in Tables 2 and 3. Moreover, the hybrid Algorithms steps for GA-PS and SA-PS are described in the following steps:

Step 1 *Initialization*: As shown in (1) and (2), the unknowns parameters are $[s_k]_{k=1}^{P}$, $[\theta_i]_{i=1}^{P}$ and $[\phi_j]_{j=1}^{P}$. Hence, we formulate M number of particles at random as shown in Table 1.

Table 1. Randomly generated M number of particles.

Amplitudes	Elevation angles	Azimuth angles
$s_{11}\, s_{12} \ldots\, s_{1P}$	$\theta_{1,P+1}\, \theta_{1,P+2} \ldots\, \theta_{1,2P}$	$\phi_{1,2P+1}\, \phi_{1,2P+2} \cdots\, \phi_{1,3P}$
$s_{21}\, s_{22} \ldots\, s_{2P}$	$\theta_{2,P+1}\, \theta_{2,P+2} \ldots\, \theta_{2,2P}$	$\phi_{2,2P+1}\, \phi_{2,2P+2} \cdots\, \phi_{2,3P}$
$s_{31}\, s_{32} \ldots\, s_{3P}$	$\theta_{3,P+1}\, \theta_{3,P+2} \ldots\, \theta_{3,2P}$	$\phi_{3,2P+1}\, \phi_{3,2P+2} \cdots\, \phi_{3,3P}$
. . .	. . .	. . .
. . .	. . .	. . .
. . .	. . .	. . .
$s_{M1}\, s_{M2} \ldots\, s_{Mp}$	$\theta_{M,P+1}\, \theta_{M,P+2} \ldots\, \theta_{M,2P}$	$\phi_{M,2P+1}\, \phi_{M,2P+2} \cdots\, \phi_{M,3P}$

Where $s_{ij} \in R : -L_s \leq s_{ij} \leq H_s$, $\forall i = 1, 2, \ldots, M$, $j = 1, 2, \ldots P$, where L_s and H_s are the lowest and highest possible limits of the signal amplitudes. Similarly,

$$\theta_{ij} \in R : 0 \leq \theta_{ij} \leq \pi/2, \ \ \forall i = 1, 2, \ldots, M, \ \ j = P+1, P+2, \ldots, 2P,$$

and

$$\phi_{ij} \in R : 0 \leq \phi_{ij} \leq 2\pi, \ \forall i{=}1, 2, \ldots, M, \ j = 2P+1, 2P+2, \ldots, 3P.$$

Step 2 *Fitness Evaluation*: Find the fitness of each particle using the fitness function given as

$$FF(i) = 1/(1 + D(i)) \tag{3}$$

where $D\,(i)$ is the difference function for ith particle and is given as

$$D(i) = D_1(i) + D_2(i)$$

where

$$D_1(i) = 1/M \sum_{x=1}^{M} |y_x - \hat{y}_x^i|^2 \tag{4}$$

and

$$D_2(i) = 1/M \sum_{z=1}^{M} |y_z - \hat{y}_z^i|^2 \tag{5}$$

y_x and y_z are given in (1) and (2), while $\hat{y}_x^i$ and $\hat{y}_z^i$ for mth elements in the array is given as follows

$$\hat{y}_{xm}^i = \sum_{k=1}^{P} \mathbf{b}_{i,P} e^{-j(m-1)\pi \sin(\mathbf{b}_{i,P+k}) \cos(\mathbf{b}_{i,2P+k})}$$

and

$$\hat{y}^i_{zm} = \sum_{k=1}^{P} \mathbf{b}_{i,P} e^{-j(m-1)\pi \cos(\mathbf{b}_{i,P+k})}$$

where b_i is shown in Table 1.

Step 3 *Termination Criteria*: The termination criteria of the algorithm is made on the following results achieved.

a) If the pre-defined fitness value is achieved $\varepsilon_j \leq 10^{-12}$.
OR

b) If the maximum number of cycles have reached.

Step 4 *Reproduction*: As given in the Tables 2 & 3, use the operators of crossover, Mutation selection and Elitism to reproduce the new population.

Step 5 *Refinement*: PS and SA algorithms are used for further tuning

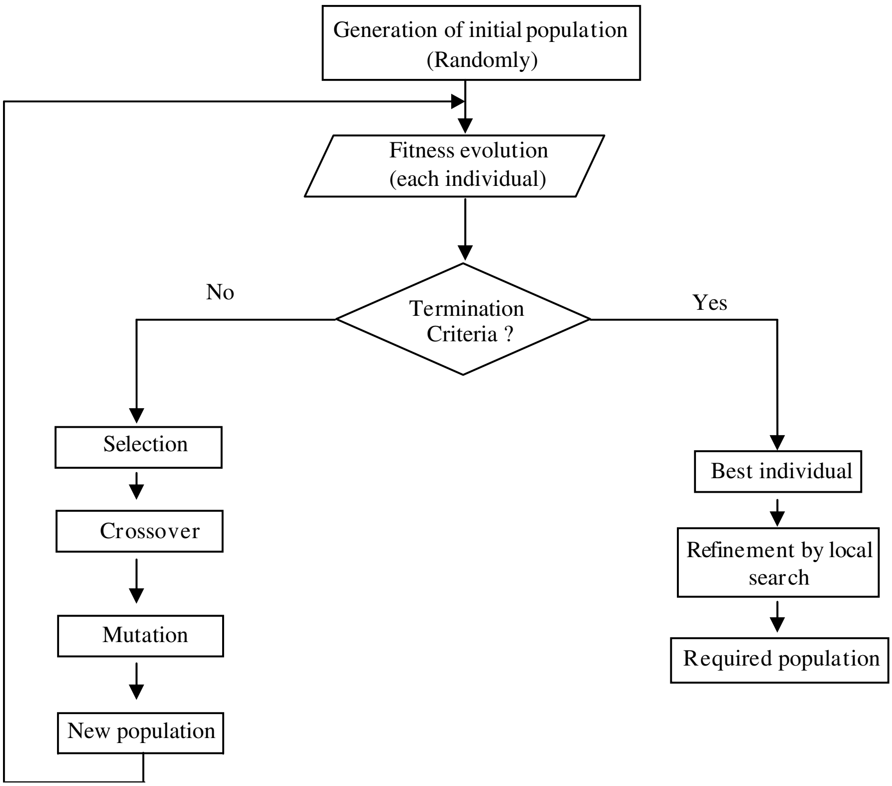

Figure 2. Generic flow diagram for intelligent hybrid computing.

Table 2. Parameters settings for GA and PS.

GA		PS	
Parameters	**Settings**	**Parameters**	**Setting**
Population size	240	Poll method	GPS Positive basis 2 *N*
No of Generation	1000	Polling order	Consecutive
Migration Direction	Both Way	Maximum iteration	800
Crossover fraction	0.2	Function Evaluation	16000
Crossover	Heuristic	Mesh size	01
Function Tolerance	10-12	Expansion factor	2.0
Initial range	[0-1]	Contraction factor	0.5
Scaling function	Rank	Penalty factor	100
Selection	Stochastic uniform	Bind Tolerance	10-03
Elite count	2	Mesh Tolerance	10-06
Mutation function	Adaptive feasible	*X* Tolerance	10-06

Table 3. Parameters settings for SA.

SA	
Parameters	**Settings**
Annealing Function	Fast
Reannealing interval	100
Temperature update function	Exponential temperature update
Initial temperature	100
Data type	Double
Function Tolerance	10–12
Max iteration	1000
Max function evaluations	3000*number of variables

of results. The best individual of GA has been given as a starting point to PS algorithm. Similarly the best individual of SA algorithm has been given as a starting point to PS algorithm.

Step 6 *Storage*: Store the global best of this cycle and repeat the steps 2 to 5 for sufficient numbers of independent runs for better statistical analysis.

4. SIMULATION AND RESULTS

In this section, various simulation results are given to jointly estimate the amplitude and direction of arrival of far field sources. We described the performance of five methods, the GA, PS, GA-PS technique, SA and SA-PS technique. We have used L-type array which is composed of two uniform linear arrays, i.e., one array is placed along X-axis and the other is placed along Z-axis. The distance between the two adjacent elements in each uniform linear array is kept half the wavelength of the signal wave, i.e., $d = \lambda/2$. The reliability and effectiveness of the proposed scheme is tested on the basis of large number of Monte-Carlo simulations by using MATLAB version 7.8.0.347. The criterion made for the joint estimation of amplitude and DOA is based on Mean Square Error (MSE) as a fitness evaluation function. The relation used for MSE is given in Eq. (4). Only a single snapshot is used throughout the simulation results and a Matlab built-in tool box "optimization of population" based algorithm is used with the setting shown in Tables 2 and 3. All the results are averaged over 50 runs.

4.1. Case I

In this subsection, the accuracy of all five techniques has been discussed. We assume two sources which are impinging on L-type array from far field. In this case, the L-type array consists of seven elements, i.e., three elements along X-axis while three elements along Z-axis. The reference element is common for both arrays. The amplitude of these two sources are denoted by s_1, and s_2 while the DOA (Elevation and azimuth angles) of arriving signals are denoted by θ_1, θ_2 and ϕ_1, ϕ_2 respectively. The s_1, θ_1, ϕ_1 correspond to the first source while s_2, θ_2, ϕ_2 correspond to the second source. Initially the performances of all five techniques are discussed in the absence of any noise in the system. We have taken $s_1 = 1$, $s_2 = 2$, $\theta_1 = 0.5236$, $\theta_2 = 0.8727$, $\phi_1 = 1.2217$, $\phi_2 = 1.9199$ as shown in Table 4. All the values of DOA of sources are taken in radians. One can see from Table 4, that all the five schemes produce fairly accurate results for joint estimation of amplitude and DOA for two sources. However, among all these techniques, the hybrid GA-PS technique is found to be the best technique as shown in Table 4. The second best is GA which produces better results for the same two sources.

Now we describe the Mean Square Error (MSE) and percentage convergence of all five schemes for joint estimation of Amplitude and DOA of two sources. We set 10^{-2} as a threshold MSE for all schemes. Initially, we have taken five elements in the L-type array, i.e., two elements along the X-axis and two elements along the Z-axis while

Table 4. Amplitude and DOA estimation of 2-sources using 7-elements L-type array.

Scheme	$\mathbf{s_1}$	$\mathbf{s_2}$	$\boldsymbol{\theta_1}$	$\boldsymbol{\theta_2}$	$\boldsymbol{\phi_1}$	$\boldsymbol{\phi_2}$
Actual values	1.0000	2.0000	0.5236	0.8727	1.2217	1.9199
GA	1.0008	2.0008	0.5234	0.8735	1.2225	1.9207
PS	1.0032	2.0033	0.5268	0.8759	1.2249	1.9231
GA-PS	1.0000	2.0000	0.5235	0.8726	1.2216	1.9198
SA	1.0196	2.0195	0.5432	0.8923	1.2413	1.9395
SA-PS	1.0063	2.0063	0.5299	0.8790	1.2281	1.9263

the reference element is common for both arrays. As shown in Table 5, the performance of the hybrid approach GA-PS is better than the other schemes in terms of convergence rate and MSE. The hybrid approach GA-PS converges 98% and the average MSE is 10^{-9}. The GA converges 95% with MSE is 10^{-7} Table 5. Moreover, the PS technique converges 80% with MSE is 10^{-4}. The convergence rate of SA algorithm is poor which is only 10% with MSE is 10^{-2}. The hybrid SA-PS algorithm converges 60% and the average MSE for this scheme is 10^{-3}. The convergence rate and MSE of all schemes are also checked for increasing number of sensors in the array. Every time we keep equal number of elements in the sub-array along the X-axis and the sub-array along the Z-axis. As shown in Table 5, that for increasing number of elements in the L-type array, the MSE and convergence rate of all schemes improves. All the above mentioned five technique fails when the number of elements are less than the number of sources as it becomes an under determined problem.

4.2. Case II

In this subsection, we discuss the performance of all five techniques for three sources. Initially, the L-type array consists of thirteen elements. The sub-array along X-axis as well as the sub-array along Z-axis consists of four elements, while the reference element is common for both sub-arrays. We take $s_1 = 1$, $s_2 = 2$, $s_3 = 3$, $\theta_1 = 0.1745$, $\theta_2 = 0.8727$, $\theta_3 = 1.3090$, and $\phi_1 = 1.3090$, $\phi_2 = 1.9199$, $\phi_3 = 2.4435$. In this case, we faced few local minima with the increase of unknowns (Sources) in the problem and due to which the performance of all schemes are degraded as compared to Case I. Table 6 shows that the hybrid approach GA-PS produces much accurate results as compared to the other four schemes for the joint estimation of amplitude and DOA of three sources. The second best result is given by GA.

Table 5. MSE and % convergence for different numbers of elements in L-type array.

No. of Elements	Scheme	MSE	% Convergence	No. of Elements	Scheme	MSE	% Convergence
5	GA	10^{-7}	95	11	GA	10^{-10}	98
	PS	10^{-4}	80		PS	10^{-7}	85
	GA-PS	10^{-9}	98		GA-PS	10^{-12}	100
	SA	10^{-2}	10		SA	10^{-5}	15
	SA-PS	10^{-3}	60		SA-PS	10^{-6}	67
7	GA	10^{-8}	97	13	GA	10^{-11}	98
	PS	10^{-5}	82		PS	10^{-7}	86
	GA-PS	10^{-10}	100		GA-PS	10^{-13}	100
	SA	10^{-3}	11		SA	10^{-5}	16
	SA-PS	10^{-4}	62		SA-PS	10^{-6}	70
9	GA	10^{-9}	98	15	GA	10^{-12}	98
	PS	10^{-6}	83		PS	10^{-8}	87
	GA-PS	10^{-11}	100		GA-PS	10^{-14}	100
	SA	10^{-4}	13		SA	10^{-6}	18
	SA-PS	10^{-5}	65		SA-PS	10^{-7}	70

Table 6. Amplitude and DOA estimation of three sources using 13-elements L-type array.

Scheme	$\mathbf{s_1}$	$\mathbf{s_2}$	$\mathbf{s_3}$	$\boldsymbol{\theta_1}$	$\boldsymbol{\theta_2}$	$\boldsymbol{\theta_3}$	$\boldsymbol{\phi_1}$	$\boldsymbol{\phi_2}$	$\boldsymbol{\phi_3}$
Assumed	1.0000	2.0000	3.0000	0.1745	0.8727	1.3090	0.5236	0.9199	2.4435
GA	1.0073	2.0073	3.0073	0.1818	0.8800	1.3163	0.5309	0.9272	2.4508
PS	1.0278	2.0277	3.0277	0.2023	0.9005	1.3368	0.5514	1.9477	2.4713
GA-PS	1.0011	2.0011	3.0011	0.1756	0.8738	1.3101	0.5247	1.9210	2.4446
SA	1.0610	2.0611	3.0610	0.2355	0.9337	1.3700	0.5846	1.9809	2.5045
SA-PS	1.0432	2.0432	3.0432	0.2177	0.9159	1.3522	0.5668	1.9631	2.4867

Now we discuss the reliability of all five schemes in terms of MSE and their rate of convergence for three sources. We set MSE 10^{-2} as threshold for all five schemes. Initially we take seven elements in the L-type array, i.e., three elements along X-axis while three elements along Z-axis. As discussed earlier, with the increase of unknowns the local minima also increases. Hence, the performance of all five techniques are also degraded in terms of MSE and their rate of convergence as shown in Table 7. In this case, the convergence rate of the hybrid approach

Table 7. MSE and % convergence for different numbers of elements in L-type array.

No. of Elements	Scheme	MSE	% Convergence	No. of Elements	Scheme	MSE	% Convergence
7	GA	10^{-6}	85	13	GA	10^{-7}	89
	PS	10^{-3}	50		PS	10^{-4}	57
	GA-PS	10^{-7}	95		GA-PS	10^{-8}	98
	SA	10^{-1}	0		SA	10^{-1}	0
	SA-PS	10^{-1}	20		SA-PS	10^{-2}	24
9	GA	10^{-7}	87	15	GA	10^{-8}	90
	PS	10^{-3}	52		PS	10^{-5}	60
	GA-PS	10^{-8}	96		GA-PS	10^{-9}	98
	SA	10^{-1}	0		SA	10^{-1}	5
	SA-PS	10^{-2}	22		SA-PS	10^{-3}	24
11	GA	10^{-7}	88	17	GA	10^{-9}	92
	PS	10^{-4}	55		PS	10^{-5}	62
	GA-PS	10^{-8}	97		GA-PS	10^{-11}	98
	SA	10^{-1}	0		SA	10^{-1}	5
	SA-PS	10^{-2}	22		SA-PS	10^{-3}	25

GA-PS is 95% with MSE is 10^{-7}. The GA has obtained second best performance among the remaining techniques with 85% convergence and MSE as 10^{-7}. However, we observed a drastic decrease in the performance of PS, SA and SA-PS in terms of their MSE and rate of convergence for joint estimation of amplitudes and DOA of three sources. The PS technique has convergence rate of 50% with MSE as 10^{-3}. The convergence of the hybrid technique SA-PS limited to 20% with MSE as 10^{-1}, while the convergence of SA algorithm is 0% with MSE as 10^{-1}. We also check the convergence and MSE for different number of sensors in the L-type array. With the increase of elements in the array, we found that the performance of these techniques improves in terms of convergence and MSE as shown in Table 7.

4.3. Case III

In this subsection, the performance of all five algorithms are discussed for the joint estimation of Amplitudes and DOA of four far field sources. Initially, the L-type array is composed of fifteen elements. The sub-array along the X-axis consists of seven elements, while the same number of elements is placed in the sub-array along Z-axis. We take

$s_1 = 1$, $s_2 = 2$, $s_3 = 3$, $s_4 = 4$, $\theta_1 = 0.2618$, $\theta_2 = 0.6109$, $\theta_3 = 1.0472$, $\theta_4 = 1.4835$ and $\phi_1 = 1.6581$, $\phi_2 = 2.1817$, $\phi_3 = 2.7925$, $\phi_4 = 3.4034$, as shown in Table 8. In this case, we have more local minima due to which the performance of all the techniques is degrade. Again, one can see from Table 8, that the hybrid approach (GA-PS) produces better results even in the presence of strong local minima. The performance of PS technique, as well as, of SA and SA-PS is affected more due to these local minima.

Now, we look at the reliability of all five schemes in terms of their convergence rate and MSE for four sources. Due to the increase in number of unknowns, the number of local minima increases. Due to more local minima's, the performance of all five techniques degraded. The threshold value of MSE is set 10^{-2}. Even in the presence of strong local minima the reliability of hybrid GA-PS approach is much better than the other four techniques. The convergence of GA-PS technique is 80% with MSE as 10^{-6}. The convergence of GA is 65% with MSE as 10^{-4} as shown in Table 9. The convergence of PS is 10% while the convergence of SA as well as SA-PS is noted to be 0%. The performance

Table 8. Amplitude and DOA estimation of four sources using 15-elements L-type.

Scheme	s_1	s_2	s_3	s_4	θ_1	θ_2	θ_3	θ_4	ϕ_1	ϕ_2	ϕ_3	ϕ_4
Assumed	1.0000	2.0000	3.0000	4.0000	0.2618	0.6109	1.0472	1.4835	1.6581	2.1817	2.7925	3.4034
GA	1.0163	2.0163	3.0162	4.0163	0.2781	0.6272	1.0635	1.4998	1.6744	2.1980	2.8088	3.4197
PS	1.0425	2.0425	3.0426	4.0426	0.3043	0.6534	1.0897	1.5260	1.7006	2.2242	2.8350	3.4468
GA-PS	1.0083	2.0083	3.0083	4.0083	0.2701	0.6192	1.0555	1.4918	1.6664	2.1900	2.8008	3.4117
SA	1.1263	2.1263	3.1263	4.1164	0.3881	0.7372	1.1735	1.6098	1.7844	2.3080	2.9188	3.5306
SA-PS	1.0932	2.0932	3.0932	4.0932	0.3550	0.7041	1.1404	1.5767	1.7513	2.2749	2.8857	3.4966

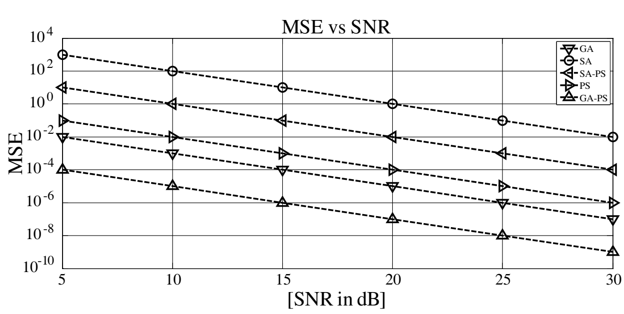

Figure 3. Mean square error vs signal to noise ratio.

Table 9. MSE and % convergence for different numbers of elements in L-type array.

No. of Elements	Scheme	MSE	% Convergence	No. of Elements	Scheme	MSE	% Convergence
9	GA	10^{-4}	65	15	GA	10^{-6}	68
	PS	10^{-1}	10		PS	10^{-2}	11
	GA-PS	10^{-6}	80		GA-PS	10^{-7}	82
	SA	10^{-1}	0		SA	10^{-1}	0
	SA-PS	10^{-1}	0		SA-PS	10^{-2}	2
11	GA	10^{-5}	66	17	GA	10^{-7}	70
	PS	10^{-1}	10		PS	10^{-2}	11
	GA-PS	10^{-7}	82		GA-PS	10^{-8}	83
	SA	10^{-1}	0		SA	10^{-1}	0
	SA-PS	10^{-1}	0		SA-PS	10^{-2}	3
13	GA	10^{-8}	70	19	GA	10^{-8}	70
	PS	10^{-3}	13		PS	10^{-3}	13
	GA-PS	10^{-9}	85		GA-PS	10^{-10}	85
	SA	10^{-1}	0		SA	10^{-1}	0
	SA-PS	10^{-2}	2		SA-PS	10^{-2}	4

of GA, GA-PS, SA-PS and PS in terms of convergence as well as MSE becomes slight better when we increase the number of elements in the array.

Now we evaluate the performance of all techniques against noise. Fig. 3 shows MSE of all techniques aginst SNR. The values of SNR is ranging from 5 dB to 30 dB while the MSE is ranging from 10^{+4} to 10^{-10}. All these curves are carried out for two sources and seven elements in the array. It has been shown in Fig. 3, that the performance of GA-PS is better then all the other techniques against all values of SNR. Secondly we have better result for GA, in terms of MSE against the different values of snr. In position three, we get a good curve for PS and at position four and five we find SA-PS and SA, respectively.

5. CONCLUSION AND FUTURE WORK

In this work, five techniques, GA, PS, Hybrid technique GA-PS, SA, and hybrid SA-PS technique have been discussed for 2-D joint estimation of amplitude and DOA of far field sources impinging on L-type array. Different cases have been considered for different numbers of sources. It has been shown that every time the hybrid approaching

GA-PS produces better results than the other four techniques. The GA-PS technique correctly estimates the amplitude and DOA up to four far field sources.

In future, we will use these techniques for the joint estimation of amplitude and DOA of near field sources.

REFERENCES

1. Zhang, X., X. Gao, and Z. Wang, "Blind paralind multiuser detection for smart antenna CDMA system over multipath fading channel," *Progress In Electromagnetics Research*, Vol. 89, 23–38, 2009.
2. Varlamos, P. K. and C. N. Capsalis, "Electronic beam steering using switched parasitic smart antenna arrays," *Progress In Electromagnetics Research*, Vol. 36, 101–119, 2002.
3. Khan, Z. U., A. Naveed, I. M. Qureshi, and F. Zaman, "Independent null steering by decoupling complex weights," *IEICE Electronics Express*, Vol. 8, No. 13, 1008–1013, 2011
4. Mouhamadou, M., P. Vaudon, and M. Rammal, "Smart antenna array patterns synthesis: Null steering and multi-user beamforming by phase control," *Progress In Electromagnetics Research*, Vol. 60, 95–106, 2006.
5. Mukhopadhyay, M., B. K. Sarkar, and A. chakrabarty, "Augmentation of anti-jam GPS system using smart antenna with a simple DOA estimation algorithm," *Progress In Electromagnetics Research*, Vol. 67, 231–249, 2007.
6. Byrne, D., M. O'Halloran, M. Glavin, and E. Jones, "Data independent radar beamforming algorithms for breast cancer detection," *Progress In Electromagnetics Research*, Vol. 107, 331–348, 2010.
7. Nishiura, T. and S. Nakamura, "Talker localization based on the combination of DOA estimation and statistical sound source identification with microphone array," *IEEE Workshop Statistical Signal Processing*, 597–600, Oct. 2003.
8. Sotiriou, A. I., P. K. Varlamos, P. T. Trakadas, and C. N. Capsalis, "Performance of a six-beam switched parasitic planar array under one path rayleigh fading environment," *Progress In Electromagnetics Research*, Vol. 62, 89–106, 2006.
9. Wang, G. M., J. M. Xin, N. N. Zheng, and A. Sano, "Two-dimensional direction estimation of coherent signals with two parallel uniform linear arrays," *IEEE Statistical Signal Processing Workshop (SSP)*, 2011.

10. Liang, J. L., X. J. Zeng, W. Y. Wang, and H. Y. Chen, "L-shaped array-based elevation and azimuth direction finding in the presence of mutual coupling," *Signal Processing*, Vol. 91, 1319–1328, 2011.
11. Liang, J. and D. Liu, "Two L-shaped array-based 2-D doas estimation in the presence of mutual coupling," *Progress In Electromagnetics Research*, Vol. 112, 273–298, 2011.
12. Goldberg, D. E., "Genetic algorithms in search, optimization and machine learning," *Addison Wesley*, Jan. 1989.
13. Wu, B., H. Chen, and Y. Wang, "DOA estimation based on RBFNN for minimum redundancy linear array (MRLA)," *AICI '09 Proceedings of the 2009 International Conference on Artificial Intelligence and Computational Intelligence*, Vol. 2, USA, 2009.
14. Pour, H. M., Z. Atlasbaf, A. Mirzaee, and M. Hakkak, "A hybrid approach involving artificial neural network and ant colony optimization for direction of arrival estimation," *Proc. IEEE, Electrical and Computer Engineering, CCECE*, Canada, 2008.
15. Zhang, T. T., "Compensation for the mutual coupling effect in uniform circular arrays for 2D DOA estimation employing the maximum likelihood technique," *IEEE Transactions on Aerospace and Electronic Systems*, Vol. 44, No. 3, 1215–1221, 2008.
16. Smith, P. and G. Bucchler, "A branching algorithm for discriminating and tracking multiple objects," *IEEE Trans. on Automat. Contr.*, Vol. 20, 101–104, 1975.
17. Sastry, C. R., E. W. Kamen, and M. Simaan, "An efficient algorithm for tracking the angles of arrival of moving targets," *IEEE Trans. on Signal Process*, Vol. 39, No. 1, 242–246, 1991.
18. Tayem, N. and H. M. Kwon, "L-shape 2-dimensional arrival angle estimation with propagator method," *IEEE Trans. on Antennas and Propag.*, 1622–1630, 2005.
19. Kirpetrick, S., C. D. Gellat, and M. P Vecchi, "Optimization by simulated annealing," *Science*, Vol. 220, No. 4598, 671–680, 1983.
20. Cerny, V., "A thermodynamical approach to the travelling salesman problem: An efficient simulation algorithm," *J. of Optim. Theory and Appl.*, Vol. 45, 41–51, 1985.
21. Granville, V., M. Krivanek, and J.-P Rasson, "Simulated annealing: A proof of convergence," *IEEE Trans. on Pattern Anal. and Mach. Intell.*, Vol. 16, No. 6, 652–656, 1994.
22. De Vicente, J., J. Lanchares, and R. Hermida, "Placement by thermodynamic simulated annealing," *Phys. Lett. A*, Vol. 317, Nos. 5–6, 415–423, 2003.

23. Torczon, V., "On the convergence of pattern search algorithms," *SIAM Journal on Optimization*, Vol. 7, No. 1, 1–25, 1997.
24. Taddy, M. A., H. K. H. Lee, G. A. Gray, and J. D. Griffin, "Bayesian guided pattern search for robust local optimization," *Technometrics*, Vol. 51, No. 4, 389–401, 2009.
25. Holland, J. H., *Adaptation in Natural and Artificial Systems*, Amazon, 1975.
26. Srinivas, M. and L. Patnaik, "Adaptive probabilities of crossover and mutation in genetic algorithms," *IEEE Trans. on Syst., Man and Cybern.*, Vol. 24, No. 4, 656–667, 1994.
27. Zhang, J., H. Chung, and W. L. Lo, "Clustering-based adaptive crossover and mutation probabilities for genetic algorithms," *IEEE Trans. on Evol. Comput.* Vol. 11, No. 3, 326–335, 2007.
28. Aarabi, P., "Genetic sensor selection enhanced independent component analysis and its applications to speech recognition," *Proc. 5th IEEE Workshop Nonlinear Signal Information Processing*, Jun. 2001.
29. Addad, B., S. Amari, and J.-J. Lesage, "Genetic algorithms for delays evaluation in networked automation systems," *Engineering Applications of Artificial Intelligence*, Vol. 24, 485–490, Elsevier, 2011.
30. Maulik, U., "Analysis of gene microarray data in a soft computing framework," *Engineering Applications of Artificial Intelligence, Elsevier, Signal Process*, Vol. 24, 485–490, 2011.